ARTICLE

Electropolymerized Tricopolymer Based on *N*-Pyrrole Derivatives as a Primer Coating for Improving the Performance of a Drug-Eluting Stent

Regina Okner,[†,‡] Yulia Shaulov,[‡] Noam Tal,[‡] Gregory Favaro,[§] Abraham J. Domb,[‡] and Daniel Mandler*[,†]

Department of Inorganic and Analytical Chemistry, The Hebrew University of Jerusalem, Jerusalem 91904, Israel, Department of Medicinal Chemistry and Natural Products, School of Pharmacy, Faculty of Medicine, The Hebrew University of Jerusalem, Jerusalem 91120, Israel, and CSM Instruments SA, Rue de la Gare 4, Peseux 2034, Switzerland

ABSTRACT The coating of medical implants by polymeric films aims at increasing their biocompatibility as well as providing a durable matrix for the controlled release of a drug. In many cases, the coating is divided into a primer layer, which bridges between the medical implant and the drug-eluting matrix. The primer coating must be very carefully designed in order to provide optimal interactions with the surface of the medical implant and the outer layer. Here we present a simple and versatile approach for designing the primer layer based on electropolymerization of a carefully chosen blend of three different pyrrole derivatives: *N*-methylpyrrole (N-me), *N*-(2-carboxyethyl)pyrrole (PPA), and the butyl ester of *N*-(2-carboxyethyl)pyrrole (BuOPy). The composition and physical properties of the primer layer were studied in detail by atomic force microscopy (AFM) and a nano scratch tester. The latter provides the in-depth analysis of the adhesion and viscoelasticity of the coating. AFM phase imaging reveals a uniform distribution of the three monomers forming rough morphology. This primer layer significantly improved the morphology, stability, and paclitaxel release profile of a paclitaxel-eluting matrix based on methyl and lauryl methacrylates.

KEYWORDS: electropolymerization • pyrrole, • stent • primer coating • adhesion • flexibility • controlled release

INTRODUCTION

Since the development of percutaneous transluminal coronary angioplasty (PTCA) in the early 1970s, it has been adopted by the medical community and in many occasions replaced the use of coronary artery bypass graft because of the simple noninvasive procedure that it requires. Despite this advantage and along with shorter recovery time, PTCA frequently has a high rate of restenosis (about 40% of the cases within 6 months). The rapid development of stent technology in the early 1990s was a huge leap forward in treating restenosis (reducing the restenosis to 20%) by providing excellent mechanical support of the vessel wall (1, 2). However, bare metal stents did not prevent restenosis occurrence after stenting, caused by local inflammation, thrombosis, and fibromuscular proliferation (2). The high incidence of short- and long-term *in stent* restenosis leads to repetition of angioplasty procedures. Many efforts have been made to coat bare metal stents with biocompatible coating (polymeric and others) using different methods to diminish their thrombogenic properties (3−7). In the late 1990s, antiproliferative drugs, such as paclitaxel and sirolimus, were incorporated for the first time into a biocompatible stent coating (8−10). Nowadays, drug-eluting stents (DESs) are replacing conventional bare stents as a major medical device for treating coronary artery disease. Boston Scientific and Johnson and Johnson (Cordis) pioneered this field and launched almost at the same time (in 2003) the first DES: Taxus and Cypher, respectively (11−18). The use of DESs was estimated to reach 87% of all angioplasty procedures by 2004 (19). Today, Taxus and Cypher DESs dominate the market according to a 2006 Federal Drug Administration (FDA) report. Although the use of polymer-based DESs has been successful in reducing the risk of *in stent* restenosis, there is still concern about the safety and integrity of the polymer layer. A number of publications dealing with problems associated with the morphology and mechanical stability of the coatings of commercially available DESs have been published (20−22). These reveal adhesion and uniformity irregularities of the coatings before and after balloon expansion. Such defects are likely to cause a potential risk of thrombosis, coronary microembolism of the polymer layer pieces, and late inflammatory or neointimal reactions.

The improvement of the mechanical properties of stent coating is currently a major scientific as well as commercial

* Corresponding author. Tel: +972 2 658 5831. Fax: +972 2 658 5319. E-mail: mandler@vms.huji.ac.il.

Received for review October 23, 2008 and accepted February 12, 2009

† Department of Inorganic and Analytical Chemistry, The Hebrew University of Jerusalem.

‡ Department of Medicinal Chemistry and Natural Products, School of Pharmacy, Faculty of Medicine, The Hebrew University of Jerusalem.

§ CSM Instruments SA.

DOI: 10.1021/am800139s

Published on Web 03/10/2009

challenge in DES development. It is well-known that the adhesion between the coating and the metal substrate is fairly poor. This is due to the lack of proper interaction between the hydrophilic oxide surface of the stent and the hydrophobic polymer−drug matrix. A number of solutions for solving this problem by changing the chemistry and morphology of the stent surface have been proposed. The FDA has already approved the use of poly(*p*-xylene) (ppx) and its derivatives (23), such as Parylene C and Parylene N, as a thin primer hydrophobic coating for medical implants (24). It has been proven that the polymer−drug matrix (biodegradable or not) has indeed better adhesion on the stent surface modified with this primer coating. This family of coatings is applied onto the surface by the chemical vapor deposition (CVD) method, which requires high temperature, low pressure, and complex equipment (25). Hence, there is a true need for a simple stent coating method for depositing the primer coating. We have already demonstrated that electrochemistry, specifically electropolymerization of conducting polymers on stainless steel, can be an attractive method for coating metallic implants (26−28). Varying the electrochemical conditions, the chemical structure of the monomers, and their ratio in the deposition solution allowed the creation of coatings with different properties (29). Our previous report focused on the general concept of coating stents electrochemically and investigating their biocompatibility and drug-releasing profile (30). Moreover, the biocompatibility and stability of coatings based on polypyrrole derivatives have also been reported by us (30). We found that the coatings were nontoxic and nonbiodegradable [by high-performance liquid chromatography (HPLC) and gel permeation chromatography inspection], and there was no visual change in their surface morphology within 8 months of exposure to a physiological medium. The pN-me mix (see below) coating was also examined by histopathology and found to be nontoxic to surrounding tissues.

Here we present electrocoating of tricopolymer (called pN-me mix) based on three *N*-pyrrole derivatives [*N*-methylpyrrole (N-me), *N*-(2-carboxyethyl)pyrrole (PPA), and the butyl ester of *N*-(2-carboxyethyl)pyrrole (BuOPy)]. This layer has been examined as a primer coating on a stent, on which a new nonbiodegradable copolymer (called pLM), based on methacrylate derivatives (MMA and LMA) as a drug carrier, was deposited (31). The pN-me mix coating was characterized by electrochemistry, contact-angle goniometry, atomic force microscopy (AFM), profilometry, and electron and optical microscopy. Furthermore, its adhesion to the stent and elasticity was measured by nano scratch testing. We find that the hydrophobicity and morphology of the primer coating match very well with those of the polymer−drug matrix. AFM measurements showed that pLM mixed with paclitaxel formed very smooth and homogeneous coating. Finally, the thin pN-me mix primer coating was superior to a bare stent in supporting the second layer of the drug−polymer matrix.

MATERIALS AND METHODS

2.1. Materials. 316L stainless steel plates (10 × 20 mm^2) were used for profilometry and contact-angle measurements of the electrodeposited polymers, while 316L stainless steel stents were applied for adhesion, flexibility, and in vitro drug release. The stents had a length of 12 mm, a surface area of ca. 49 mm^2, and a closed diameter of 1.8 mm (both plates and stents were produced by STI Laser Industries Ltd., Or-Akiva, Israel). Paclitaxel was purchased from Sigma-Aldrich (St. Louis, MO).

N-Methylpyrrole (N-me) was distilled from a commercially available product obtained from Sigma-Aldrich and stored under argon prior to use. ^{1}H NMR ($CDCl_3$): δ 6.77 (t, 2H, CH-β), 6.33 (t, 2H, CH-α), 3.80 (s, 3H, N-CH_3).

N-(2-Carboxyethyl)pyrrole (PPA) and the butyl ester of *N*-(2-carboxyethyl)pyrrole (BuOPy) were synthesized according to the procedure previously described (27). PPA. ^{1}H NMR ($CDCl_3$): δ 6.68 (t, 2H, CH-β), 6.15 (t, 2H, CH-α), 4.21 (t, 2H, N-CH_2), 2.82 (t, 2H, CH_2COO). FTIR (NaCl): 3108, 2949, 1705, 1502, 1208 cm^{-1}. Elem anal. Found: C, 60.33 (calcd 60.42); H, 6.70 (calcd 6.52); N, 9.99 (calcd 10.07). BuOPy.^{1}H NMR ($CDCl_3$): δ 6.66 (t, 2H, CH-β), 6.13 (t, 2H, CH-α), 4.21 (t, 2H, N-CH_2), 4.09 (t, 2H, $COOCH_2$), 2.76 (t, 2H, CH_2COO), 1.59 (m, 2H, COO-CH_2-CH_2), 1.35 (m, 2H, COO-CH_2-CH_2-CH_2), 0.92 (t, 3H, CH_3). FTIR (NaCl): 3095, 2959, 1734, 1500, 1167, 1090, 724 cm^{-1}. Elem anal. Found: C, 67.50 (calcd 68.02); H, 8.83 (calcd 8.78); N, 7.07 (calcd 7.16). Prepared monomers were kept at −4 °C in the dark under nitrogen.

Tetrabutylammonium tetrafluoroborate (Bu_4NF_4B) and other reagents were obtained from Sigma-Aldrich and used without further purification. Sodium dodecylsulfate (SDS), disodium hydrogen phosphate, and sodium dihydrogen phosphate were purchased from Reidel-de Haën (Seelze, Germany), whereas ethyl acetate (EtAc) and acetonitrile (ACN) were purchased from BioLab (Jerusalem, Israel). All aqueous solutions were prepared from deionized water (Barnstead Easy pure UV system). Poly(lauryl/methyl methacrylate) (bulk molar ratio 7:3; pLM) with an average molecular weight of 145.7 kDa, a polydispersity of 1.59, and T_g of −13 °C was synthesized in our laboratory (31). All other materials were of analytical grade.

2.2. Methods. 2.2.1. ***Surface Pretreatment and Analysis.*** The stent surface was pretreated with carborundum (silicon carbide) powder (32). A polishing mixture was prepared by mixing equal volumetric amounts of carborundum powders of 220, 500, and 1000 mesh. Stents were immersed in a 20 mL flask containing 10 mL of ethanol (absolute) at 60 °C and 1.5 g of the carborundum mixture. The flask was corked and placed in an ultrasonic bath for 1 h. Then the stents were washed with ethanol several times until no carborundum powder could be detected on the stents by optical microscopy. The excess of the solvent was removed with a gentle flow of dry nitrogen. X-ray photoelectron spectroscopy (XPS; Kratos Analytical, Manchester, U.K.), with an Axis Ultra spectrometer and Mg Kα radiation of 1486.71 eV, was used for surface composition analysis of stainless steel samples before and after pretreatment. Data were collected and analyzed by a vision processing program.

2.2.2. ***Electropolymerization of N-Pyrrole Derivatives.*** Electrochemical measurements were conducted with a 630B electrochemical analyzer (CH Instruments, Austin, TX) using a three-electrode cell with Ag/AgBr as the reference electrode and a platinum wire as the counter electrode. The working electrodes were 316L stainless steel plates and stents. *N*-Polypyrrole (PPy) derivatives were electrochemically deposited on the electrode surface by cycling the potential (cyclic voltammetry) in 0.1 M Bu_4NF_4B and 0.1 M total concentration of the monomers in a ACN solution. Specifically, the tricopolymer (pN-me mix) was electrodeposited from a solution consisting of BuOPy/PPA/N-me in a 7:1:2 molar ratio. A potential sweep (five scans) was applied between −0.4 and 1.4 V vs Ag/AgBr at a scan rate

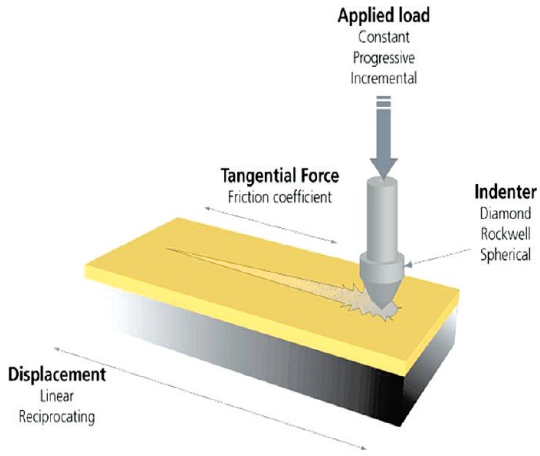

FIGURE 1. Test principle and main elements involved in the scratch test.

of 0.1 V · s^{-1}. The coated surfaces were rinsed with pure ACN and dried with a gentle stream of nitrogen.

2.2.3. *Water Contact Angle.* Contact angles were measured with a Ramé-Hart model 100 contact-angle goniometer equipped with *Dropimage* software. These measurements were repeated three times for each sample, and the average values were reported.

2.2.4. *Profilometry.* The thicknesses of the pure and drug-loaded polymer coatings were determined by a P-15 profilometer (KLA-Tencor Co., San Jose, CA). Specifically, the profiles were recorded across a notch in the coating, which was manually scratched by a wooden stick.

2.2.5. *Nano Scratch Test (NST).* The adhesive and elastic properties of stent coatings were evaluated using a CSM Nano Scratch Tester (CSM Instruments SA, Peseux, Switzerland) equipped with a diamond Rockwell tip (radius 10 μm). Scratch testing is a versatile tool for evaluating the adherence, stress, and strain between a coating and a substrate as a diamond stylus is passed across the surface while increasing the applied normal load. The mechanical response can be measured by simultaneously recording the tangential frictional force, acoustic emissions, and changes in the surface morphology while this scratch on the test surface is formed. The principle of the method and the characteristic elements involved in the scratch process are shown in Figure 1.

A progressive normal force (Fn) was applied from 0.5 to 20 mN. The pre- and postscan modes of the NST have been used for plotting the penetration and residual depth (Pd and Rd, respectively), allowing evaluation of the level of viscoelastic recovery of the samples after scratching.

2.2.6. *Flexural Strength of pLM.* The flexural strength was determined using an international testing machine (Instron 4502) equipped with a load cell of 10 N moving with a crosshead speed of 20 mm · min^{-1}. The flexural strength and flexural modulus were calculated using *Instron* software. Films were prepared by casting a copolymer solution (5 wt % in 16 mL of dichloromethane) in a 55-mm-diameter glass dish coated with Teflon paper. Dishes were covered with perforated aluminum paper, while the solvent was evaporated overnight at room temperature. Colorless, transparent smooth films were obtained and easily removed from the plates. Polymer strips (40 × 5 × 0.28 mm, $n = 4$) were die-cut from the round cast films.

2.2.7. *Surface Inspection by Scanning Electron Microscopy (SEM) and Optical Microscopy.* The morphology of the coated stents was characterized by an analytical Quanta 200 environmental scanning electron microscope (FEI Company). Coated stents were sputter-coated with a very thin Au/Pd layer using a Polaron SC7640 sputter coater. Optical microscopy was performed with an Olympus BX6000 microscope (Tokyo, Japan).

2.2.8. *Drug Loading and Release Conditions.* For in vitro release, three types of paclitaxel-loaded stents were prepared. The first type involved coating of a bare metal stent with pLM/pacliaxel (1:1, w/w). The second was a pN-me mix coated stent coated with pLM/paclitaxel (1:1, w/w), while the third type was similar to the second type, however, included a top layer of a thin drug-free pLM (1 % w/v in *n*-hexane). The pLM/paclitaxel solution was prepared in EtAc with a total concentration of 4 % (w/v).

Controlled-release experiments were carried out by incubating coated stents in a 1 mL phosphate buffer solution (0.1 M, pH 7.4) and 0.3 wt % SDS at 37 °C. At defined time intervals, the entire incubated solution was removed (and tested for the released paclitaxel amount) and replaced by a fresh buffer solution.

The total loading of paclitaxel in a stent coating was determined following an extraction protocol developed in our laboratory. Specifically, the pLM/paclitaxel coating was dissolved in 0.5 mL of chloroform. A total of 10 mL of ACN/water (6:4, v/v) was added, and the mixture was stirred and allowed to phase separate (33). As a result, the water-insoluble paclitaxel (solubility in water is less than 1 μL · mL^{-1}) (34) was transferred to the organic phase while the pLM polymer accumulated at the interface. The drug was detected by injecting 20 μL aliquots of the organic phase into the Hewlett-Packard high-performance liquid chromatograph equipped with a DAD system. Figure 2 represents a typical HPLC chromatogram obtained after extraction.

RESULTS AND DISCUSSION

3.1. Electrodeposition and Characterization of pN-me Mix. *3.1.1. Stent Surface Pretreatment.* One of the most significant parameters in developing coatings for stents is the adhesion of the layer to the stent. Adhesion depends on the interactions between the coating and the stent surface. It is well-known that adhesion of an organic polymer bearing oxygen functionalities is better on oxidized surfaces (35). For example, the electrodeposition of PPy from aqueous solutions containing oxalic acid on an oxidized iron surface leads to an adhesive polypyrrole oxalate (PPy-Ox) composite film. The strong adhesion of the composite PPy-Ox is mainly caused by an interlayer of iron oxalate formed at the interface between Fe and PPy-Ox. Yet, the PPy-Ox layer exhibited high hardness and low electrical conductivity presumably because of its nonporous bulk structure (36). In addition, electrodeposition of hydrophobic pyrrole derivatives in aqueous media is limited.

The surface of 316L stainless steel is covered by heterogeneous chromium oxide, Cr_2O_3, along with elemental iron and nickel and their respective oxides. This coating, which enhances corrosion protection, is usually improved by electropolishing (especially of the stent surfaces) because of an increase of the Cr/Fe surface ratio (37, 38). Moreover, electropolishing results in a smoother surface, which quite often decreases adhesion of the organic coating.

Indeed, we found that the various surface pretreatment procedures consisting of rearrangement of the oxide layer by either electropolishing or acid treatment did not improve adhesion of the *N*-pyrrole derivatives. On the other hand, mechanical polishing, which increases the surface rough-

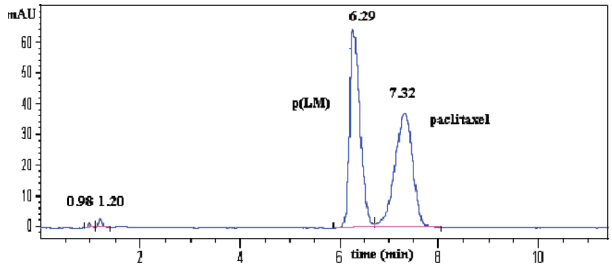

FIGURE 2. Separation of paclitaxel and pLM by HPLC on a C18 reverse-phase column over 15 min at a flow rate of 1 mL · min^{-1}.

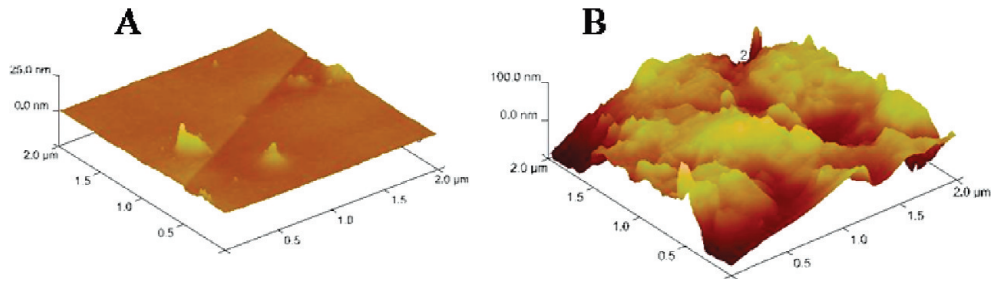

FIGURE 3. Three-dimensional AFM images of a stent before (A) and after (B) carborundum treatment.

Scheme 1. Chemical Structures of PPA, BuOPy, and N-me

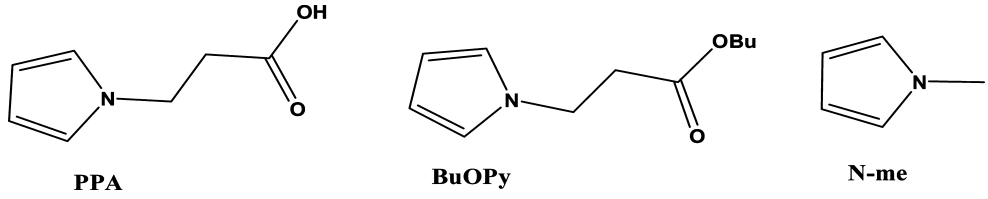

ness, might be an alternative pretreatment of stents as a means of increasing adhesion of a coating. Hence, we decided to treat the stent with carborundum powder. This treatment decreased the Cr/Fe surface ratio from 0.67 (before) to 0.38 (after), whereas the chromium oxide to chromium (Cr_2O_3/Cr) ratio increased from 7.3 (before) to 19 (after). The elemental ratio between chromium and its different oxidation states and iron was determined by XPS. These changes were accompanied by a roughness increase from 1.18 to 28.6 nm, as shown in Figure 3, which indeed improved adhesion of the pN-me mix polymer. It is worth mentioning that the surface roughness after mechanical polishing was still lower than that of the common commercial stents that are used nowadays. For example, the bare stents used by Cordis Corp. had an average root-mean-square (rms) roughness of 163 ± 44 nm (39), while our stents (produced by STI Laser Industries Ltd.) after SiC treatment reached an average rms roughness of 29 nm. Hence, we believe that our adhesion tests are relevant and, moreover, we will achieve even better results if the primer coating is applied to commercial Cypher stents.

3.1.2. Electrodeposition of a Primary Layer: pN-me Mix. According to our previous report, electrocopolymerization of mixtures of *N*-pyrrole derivatives resulted in the formation of a tricopolymer with homogeneous distribution of the components inside the film (29). The chemical composition of the individual as well as the copolymers, such as pPPA and p(PPA/BuOPy) and pBuOPy, was accomplished by different surface techniques, e.g., FTIR and XPS (29, 30). We showed that the physical and chemical properties of the copolymers are primarily controlled by the ratio of the monomers in the deposition solution, duration of electrocopolymerization, and electrochemical conditions. In this study, the stents were coated from a 0.1 M Bu_4NF_4B solution containing a mixture of 0.07 M BuOPy, 0.01 M PPA, and 0.02 M N-me. The chemical structure of the three *N*-pyrrole derivatives is shown in Scheme 1.

Typical cyclic voltammetry of electrodeposition of pN-me mix is shown in Figure 4. Five subsequent potential cycles are shown. The growth of the polymer is evident by the continuous increase of the doping and undoping waves at 0.69 V. The monomers are electrochemically oxidized at potentials more positive than 1 V, whereas the doping and

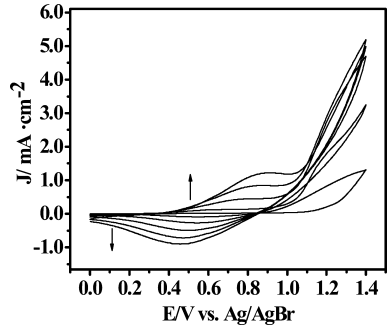

FIGURE 4. Cyclic voltammetry of 0.07 M BuOPy, 0.01 M PPA, and 0.02 M N-me in 0.1 M of Bu_4NF_4B in ACN recorded with a stent as a working electrode (the scan rate was 0.1 V · s^{-1}).

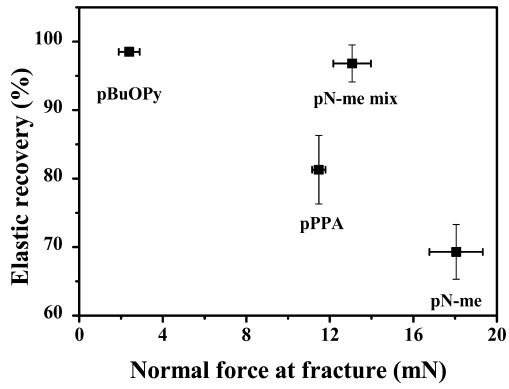

FIGURE 5. Elastic recovery after total relaxation, plotted versus the normal force at fracture.

Table 1. Physical Properties of Electrodeposited pN-me, pPPA, BuOPy, and pN-me Mix

polymer[a] composition	contact angle (deg)	thickness[b] (μm) by profilometry	thickness[c] (μm) by NST
pPPA	35 ± 5.0	0.4 ± 0.26	0.87 ± 0.02
pBuOPy	90 ± 7.7	1.8 ± 0.10	1.52 ± 0.01
pN-me	55 ± 3.8	1.5 ± 0.18	1.49 ± 0.08
N-me mix	60 ± 4.0	0.8 ± 0.07	0.87 ± 0.06

[a] The films were deposited by the application of a potential sweep between 0.4 and 1.4 V five times versus Ag/AgBr at a scan rate of 0.1 $V \cdot s^{-1}$. [b] Measured on stainless steel plates. [c] Measured on stents.

undoping processes refer to oxidation and reduction of the polymer involving the ingress and egress of ions.

3.1.3. Physical and Mechanical Properties of a Primer Layer of pN-me Mix. Adhesion and viscoelastic properties of the films were evaluated from NST (40). The latter provides viscoelastic recovery, which is indicative of deformation of the film as a result of the application of a continuously increasing force. It should be noted that viscoelastic recovery is determined after the film has completely relaxed from the scratching event. Obviously, the higher the viscoelastic recovery of the film is, the smaller the permanent deformation. Moreover, the test provides also the so-called normal force at fracture (in mN), which is the force applied to the tip at the moment of film rupture. The higher the normal force at fracture is, the better the adhesion of the film to the metal surface. Figure 5 shows the elastic recovery of the films versus the normal force at fracture for four different films using a diamond tip. It is evident that the desirable films are those located in the right higher corner of this graph.

Before any conclusion is drawn from the data presented in Figure 5, it is better to consider also the measurements summarized in Table 1, which characterize the hydrophobicity and thickness of the various components and the tricopolymer.

Table 1 presents the contact angle of a sessile water drop placed on the electrochemically coated stainless steel plates. Furthermore, the thickness of the layers was measured on plates (by profilometry) as well as on coated stents (by NST). It can be seen that the butyl ester residue (pBuOpy, which constitutes 70% of the total monomer content) provides high hydrophobicity, which creates a superior interface for the hydrophobic polymer–drug matrix (the contact angle of a pLM/paclitaxel matrix is 92° vide infra). Moreover, this monomer has excellent elasticity but poor adhesion to the surface (as is shown in Figure 5). On the other hand, pN-me has low hydrophobicity (Table 1), rigid structure, but very good adhesion to the surface (Figure 5). Therefore, we added 20% of N-me to the tricopolymer. The last component, PPA, was added in spite of the fact that it has low hydrophobicity (Table 1) and medium elasticity and adhesion (Figure 5) because of the above-mentioned claim that polymers bearing oxygen functionality adhere better to oxide surfaces. A small percent (10%) of PPA, which contains carboxylic groups, was added. Indeed, the resultant tricopolymer showed reasonable hydrophobicity (contact angle of 60 ± 4.0°), superior elasticity (96.8 ± 2.7%), and satisfactory adhesion to the stent (13.07 ± 0.9 mN). These values are a good compromise between the three properties, which we found essential for obtaining a good and stable coating. Hence, it can be concluded that, through careful blending the three monomers and because of the fact that they electropolymerize under the same conditions, it is possible to tailor the mechanical properties of the resulting polymer. Such tailoring is usually not achieved by employing a homopolymer.

Considering the thickness of the polymers, there is a good correlation between the results obtained by both methods (profilometry and NST) besides that of pPPA. We recall that the polymers were deposited under the same conditions; however, the different substrates, i.e., plate versus stent, might have an effect on polymerization. The variations in the thicknesses of the individual polymers and the tricopolymer are due to the electrochemical deposition mechanism, which was described in detail previously (29). In essence, we found that BuOPy forms thicker polymers because of an instantaneous nucleation and growth mechanism, whereas PPA forms thinner and smoother layers as a result of a progressive deposition mechanism.

AFM imaging discloses the bulk distribution of the monomers. AFM phase imaging of homopolymers, such as pPPA and pBuOPy has been previously reported (29) and proven to be an excellent tool for imaging of the individual components of the surface with high resolution. Figure 6 shows topography and phase images of pN-me mix. The phase image (Figure 6B) shows small features, where the contrast is due to grain boundaries. Focusing (Figure 6C) on each of these grains does not show phase changes that are greater than 10° [Figure 6D (1–3)]. This implies that the film is homogenously composed (with the resolution of the AFM) of the three monomers.

3.2. Second Layer of pLM/Paclitaxel and Its Interaction with the Primary Layer of the pN-me Mix Coating. *3.2.1. Physical Properties of pLM and pLM/paclitaxel Matrix.* One of the most successfully tested DESs is coated with poly(*n*-butyl methacrylate) and poly(ethylene–vinyl acetate) (Cypher). The use

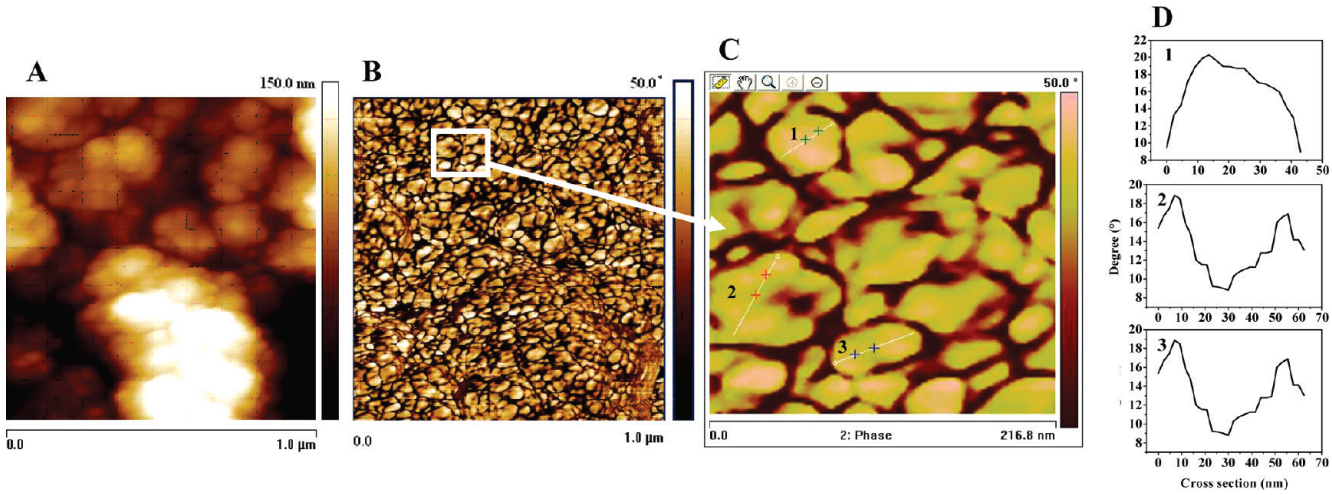

FIGURE 6. Tapping mode (A) and phase (B) imaging of the tricopolymer pN-me mix. Zoom of the phase image (C) and three cross-sectional areas of the phase image (D, 1−3).

Table 2. Mechanical Properties of pLM: Pure Copolymer and a 1:1 (w/w) Mixture with Paclitaxel

physical parameters	pLM	pLM/paclitaxel
ultimate tensile strength (MPa)	1.38 ± 0.22	1.04 ± 0.28
tensile modulus (MPa)	8.56 ± 3.29	80.00 ± 2.43
tensile elongation (%)	545.15 ± 45.90	180.03 ± 43.14
contact angle (deg)	95.6 ± 0.5	92.0 ± 0.6

of copolymers allows one to obtain different physical properties that depend on the ratio and nature of the monomers in the copolymer. pLM was synthesized in our laboratory and found to be applicable for clinical use, especially in orthopedics (31). Different bulk ratios of this copolymer were examined for stent application, considering the optimal mechanical properties, such as the ultimate tensile strength and tensile elongation. pLM with a mole ratio of 7:3 between the lauryl and methyl components gave the largest elongation and was sufficiently strong to endure the stent expansion conditions. The mechanical properties of this film with [1:1 (w/w) pLM/paclitaxel] and without paclitaxel are compared in Table 2. This polymer to drug ratio also enabled us to reach the common demand of loading 1 $\mu g \cdot mm^{-2}$ of drug per stent unit (12).

Typical stress−strain curves are presented in Figure 7. The important parameter is the elongation of the film that

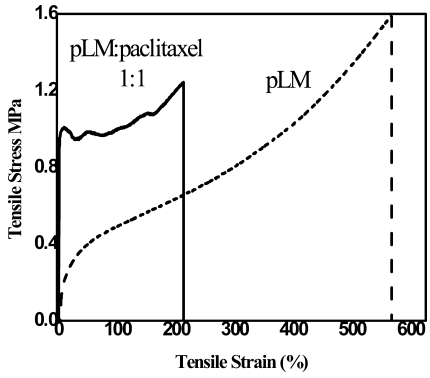

FIGURE 7. Stress−strain curves of pLM and pLM/paclitaxel (1:1, w/w) films.

occurs during stent expansion. The average stent expansion is about 200% (according to the stent initial and lumen diameters), while the single strut deformation stands on 25% (41). It can be seen from Figure 7 and Table 2 that the maximal elongation of the pLM film is more than 500% with a relatively low tensile modulus of 8.56 MPa, suggesting a soft and elastic material. The mixture of pLM with paclitaxel reduces more than twice the flexibility of the film and increases the tensile modulus 10-fold but still keeps the film suitable for stent expansion.

3.2.2. Stent Coating and Expansion. pN-me mix was electrodeposited onto a stent as a primer coating followed by dip-coating of pLM (2%)/paclitaxel (2%) (w/v) from an EtAc solution. The morphology of the coatings was investigated by AFM and SEM (Figures 8−10). The topography and cross section of the coatings obtained by AFM are shown in Figure 8. It is evident that while the primer coating (Figure 8A) is very rough ($R_q = 41.8$ nm), the secondary layer (Figure 8B), which is 0.2 μm thick, smooths out the surface significantly ($R_q = 0.4$ nm).

Smoothing of the surface can be explained by a leveling effect, namely, by filling the rough topography of the primer layer by the second layer, which results in superior adhesion vide infra.

It is well-known that a smooth stent surface reduces protein adsorption, which is a major precursor of platelet adhesion (42−44). Figure 9 represents SEM images of pLM coating on bare (A) and pN-me mix coated (B) surfaces. It can be seen that the highly rough pN-me mix primer coating provides a better substrate (as compared with bare stainless steel) for the polymer−drug matrix. It is evident from the SEM images that the polymer−drug forms a more continuous and homogeneous matrix. This is likely to be attributed to the interactions between the two polymer layers. Light microscopy images of the bare (Figure 9C) and pN-me mix (Figure 9D) coated with pLM/paclitaxel films show also the effect of the primer layer. The stent that was not coated with the primer layer (Figure 9C) shows two distinct areas that differ considerably in the coating thickness. The bright areas

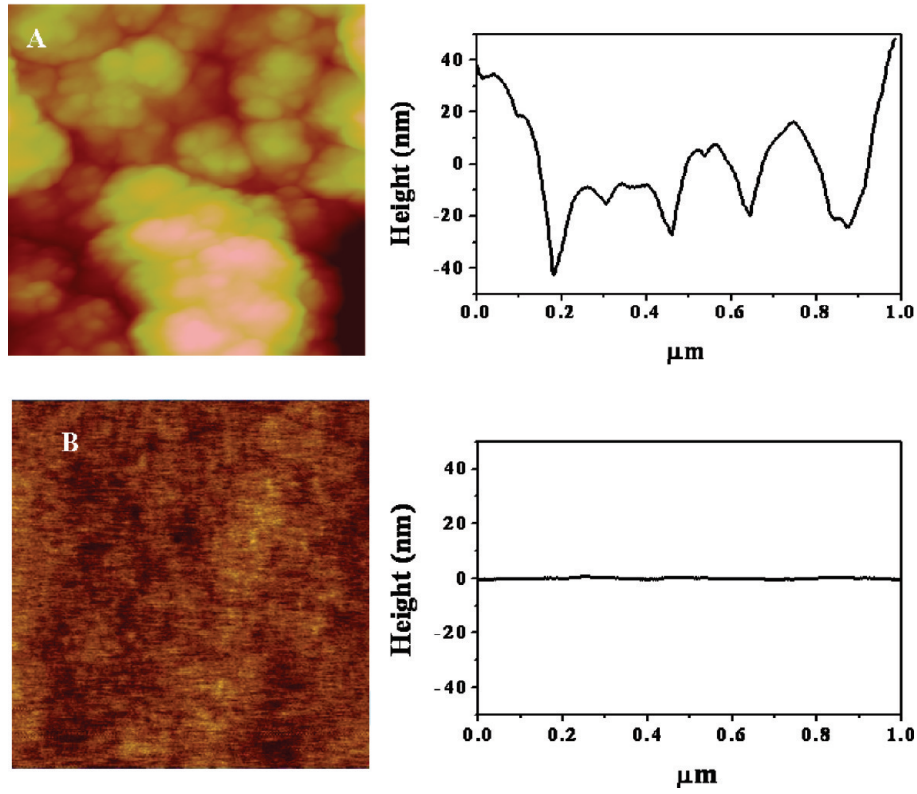

FIGURE 8. AFM topographic images and cross sections of pN-me mix (A) and pLM/paclitaxel on pN-me mix (B).

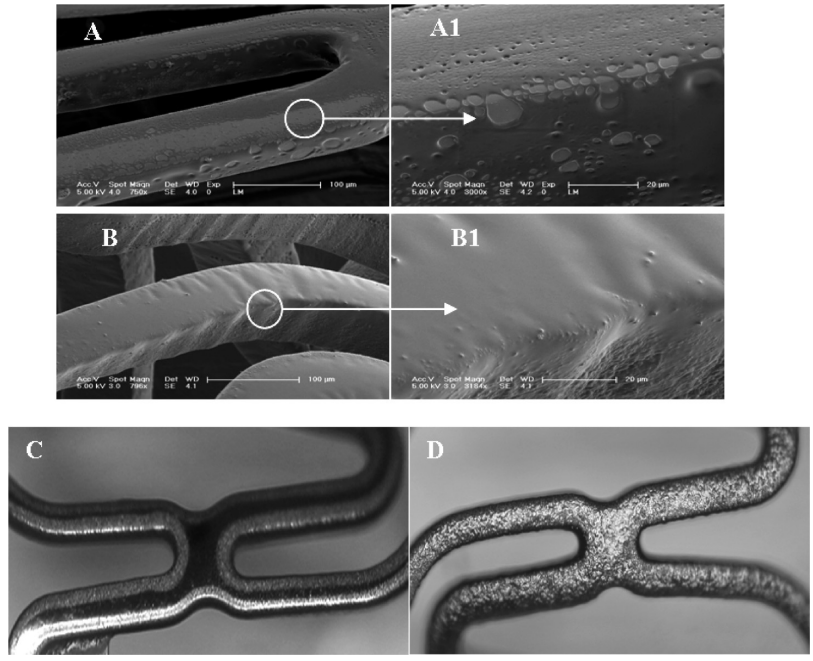

FIGURE 9. Comparison of a pLM/paclitaxel coating on a bare stent and on a pN-me mix coated stent. SEM images of pLM/paclitaxel on a bare stent (A and A1 magnifications of 750× and 3000×, respectively) and on pN-me mix (B and B1 magnifications of 750× and 3000×, respectively). Light microscopy of pLM/paclitaxel on a bare stent and on pN-me mix (C and D magnifications of 100×).

represent the thinner and rougher areas, while the darker areas are thicker and smoother. This inhomogeneity is caused by surface tension. On the other hand, the presence of the primer coating diminishes these effects and results in a uniform and smooth layer (Figure 9D). It should be noticed that the coating in Figure 9D looks rough, which is a result of the transparency of the second layer.

To mimic the real mechanical stress, which is applied on the coated stent in the course of balloon expansion, and examine the flexibility and stability of the coating, the stent was immersed into a buffer phosphate solution for 1 min and then expanded from 1.8 to 3 mm. The expanded stent surfaces were investigated by SEM (Figure 10). It can be seen that the coating is resistant to expansion because there is

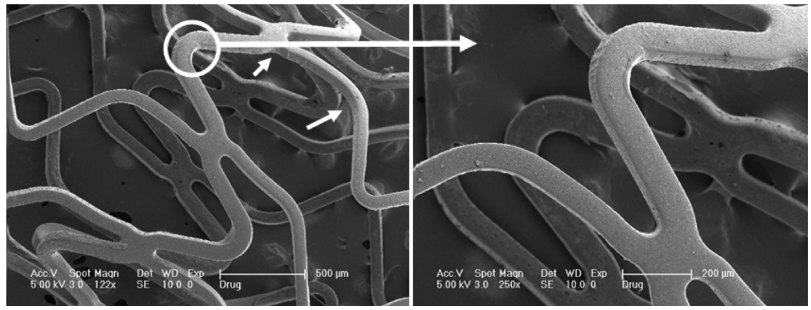

FIGURE 10. SEM images of stent coated with pN-me mix and pLM/paclitaxel (1:1). The stent was expanded to an inner diameter of 3 mm. Figure magnifications of 122× (left) and 250× (right).

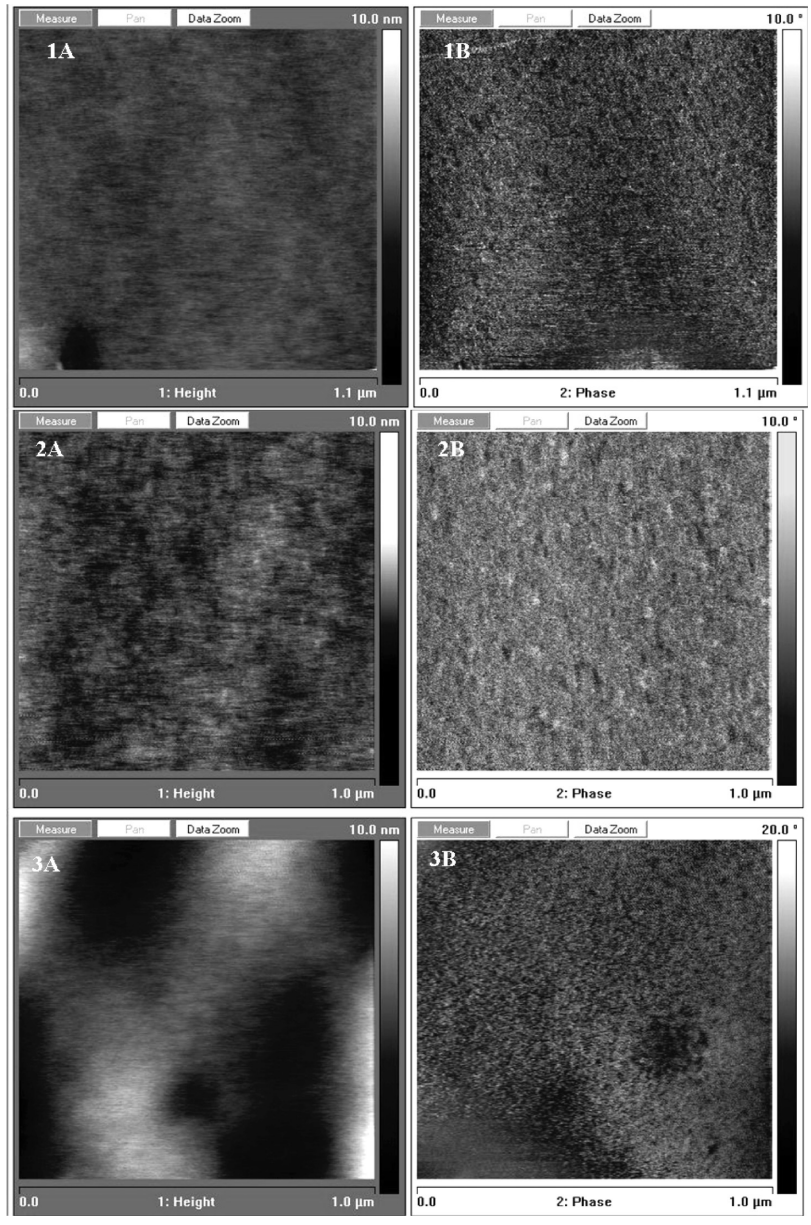

FIGURE 11. High-resolution 1 μm tapping (1A−3A) and phase (1B−3B) mode AFM images of a stent surface coated with (1) pLM film, (2) pLM/paclitaxel (1:1), and (3) pLM/paclitaxel after 24 h of incubation in the release medium.

no indication of polymer delamination or cracking at the most expanded sites (indicated with the arrows).

3.2.3. Drug Release of an in Vitro Model. Drug distribution inside pLM was investigated by phase-mode AFM. Figure 11 shows the tapping and phase modes of a pLM film without (Figure 11, 1A and 1B) and with paclitaxel (Figure 11, 2A and 2B). The pLM without the drug resulted in a homogeneous film, even though it contains two different ester groups, which are indistinguishable by this mode of AFM. The phase mode of pLM with the drug shows a similar

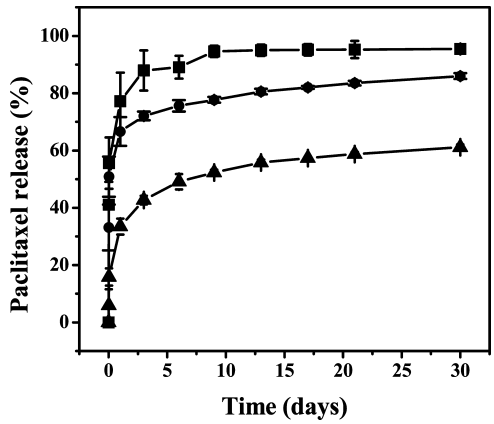

FIGURE 12. Release of paclitaxel from stents coated with pLM/paclitaxel (1:1) on a bare stent (■), pLM/paclitaxel (1:1) on a pN-me mix primer coating (●), and a diffusion-controlled system (▲) (see the Experimental Section).

image, except some bright points on the order of a few nanometers are observed (Figure 11, 2B). This suggests that not only is paclitaxel dissolved inside pLM but it is also possible that it forms small crystallites on the surface. It is well-known that paclitaxel usually recrystallizes upon solvent evaporation (33). In general, it can be concluded that the polymer and the drug form a homogeneous phase. This is in contrast to the Taxus DES in which paclitaxel is embedded inside the coating as relatively large particles (45). Parts 3A and 3B of Figure 11 show the phase-mode AFM image of a coated stent after a 24 h release experiment. The crystalline paclitaxel, which was on the surface, was dissolved, leaving the matrix without apparent morphological changes.

3.3. Drug Release. Paclitaxel release from the coated stents was investigated by monitoring the levels of the drug in the eluting buffer. The total amount of drug that was loaded onto the stent was 53 ± 7 μg, which was measured by adding the amount of drug that was released to the amount of drug that was left on the stent and determined by dissolving it later. Three drug release systems were examined: pLM/paclitaxel on a bare stent (first system), the same matrix on a pN-me mix primer coating (second system), and the latter system coated with an additional third diffusion-controlled layer (third system; see the Experimental Section) (21). The last DES is analogous to the Cypher stent (46). Figure 12 shows the release profiles for 30 days. Clear differences between the three systems are noticeable. A total of 55% of the drug was released from the first system (without a primer layer) within the first 3 h, which is similar to the percent that was released from the second system. This might be explained by the paclitaxel that is on the surface and is not likely to be affected by structural effects induced by the primer coating. On the other hand, the second system releases almost 20% less drug in the following 30 days. This difference can be attributed to surface irregularities, which were indicated by SEM analysis (Figure 9A,B). Namely, the pLM/paclitaxel coating on a bare stent is not uniform and stable and therefore detaches, which accelerates paclitaxel release. The third system succeeds in minimizing the burst release to 20% and slows down the release rate. As a result, more than 50% of the total paclitaxel content remained on the stent after 1 month. Clearly, the pLM/paclitaxel on pN-me mix assembly shows a release profile similar to that of the diffusion-controlled system after the burst. This means that the addition of a thin top layer retards the initial release of the paclitaxel that is on the pLM surface.

CONCLUSIONS

This study focuses on electrochemical deposition of a primer coating on a stainless steel stent, which was formed by the blending of three *N*-pyrrole derivatives: N-me, PPA, and BuOPy. The mechanical properties of the homopolymers and the tricopolymer (pN-me mix: 2:1:7 N-me/PPA/BuOPy) were carefully characterized using different surface techniques and, in particular, by NST. This method provides invaluable information about adhesion to the surface and, at the same time, the flexural behavior of the coating. Thus, we have clearly demonstrated that the mechanical properties of the coating can be fine-tuned by appropriately choosing the optimal combination of monomers. Each of them contributed to the final properties of the tricopolymer due to its homogeneous structure on the nanometer scale. Eventually, the pN-me mix tricopolymer showed excellent adhesion and flexibility to the stent surface. The thickness of the electrodeposited film could be controlled by the duration of electropolymerization.

pN-me mix was examined as a primer coating for a drug release matrix (pLM/paclitaxel). The double coating described here has a potential application as a drug-eluting system because of the rough morphology of pN-me mix, which functions as a good support for the pLM/paclitaxel matrix. AFM and SEM analysis disclosed a smooth and homogeneous stent coating that is resistant toward stent expansion. Furthermore, the double coating allows the extended release of paclitaxel for more than 1 month. This double coating can solve the current major DES problem of coating irregularity and delamination.

Finally, it is interesting to compare our results with previously reported DES (24, 25, 47), although such a comparison is not simple because of the fact that the morphology of many of these systems has not been described. Most commercial DESs use ppx derivatives as a primer coating applied by CVD. This coating was found to be biocompatible and biostable and was approved by the FDA. One of the studies that described the interaction between the stent surface (made of the alloy Nitinol) and this use ppx derivatives primer coating was carried out by Lahann et al. (25). The authors claimed that the superior adhesion of the primer coating was achieved by a synergistic effect between the relatively rough Nitinol surface (although the value is not mentioned) and the rigid structure of use ppx derivatives. Hanefeld and co-workers (24) demonstrated also a DES system based on a ppx primer layer. They carried out Blister tests for each of the layers and found good adhesion of ppx to the stent; however, they did not relate it to the roughness of the stainless steel. Wolf et al. (39) focused their research on the adhesion between polymer layers of a Cypher stent. The roughness of an untreated stainless steel

stent was 163 ± 44 nm, which is significantly higher than that of the mechanically polished stents used in this study.

Hence, to conclude, the approach presented here aims to provide the tools for increasing the matching between the primer- and drug-containing layers by carefully studying and tuning the nanomechanical properties of both layers.

Acknowledgment. This work was supported by The Hebrew University of Jerusalem through an applied grant and by Elutex Ltd. The Harvey M. Krueger Family Center for Nanoscience and Nanotechnology of The Hebrew University of Jerusalem is acknowledged. We are indebted to H. Harel for performing the Instron measurements.

REFERENCES AND NOTES

(1) Zimmer, S. *The Medical Device Handbook*; Deutsche Bank Securities, Inc.: Frankfurt am Main, Germany, 2002; p 8.
(2) Wang, F. W.; Stouffer, G. A.; Waxman, S.; Uretsky, B. F. *Catheter. Cardiovasc. Interv.* **2002**, *55* (2), 142.
(3) Descheerder, I. K.; Wilczek, K. L.; Verbeken, E. V.; Vandorpe, J.; Lan, P. N.; Schacht, E.; Degeest, H.; Piessens, J. *Atherosclerosis* **1995**, *114* (1), 105.
(4) Peng, T.; Gibula, P.; Yao, K. D.; Goosen, M. F. A. *Biomaterials* **1996**, *17* (7), 685.
(5) Van Der Giessen, W. J.; Lincoff, A. M.; Schwartz, R. S.; Vanbeusekom, H. M. M.; Serruys, P. W.; Holmes, D. R.; Ellis, S. G.; Topol, E. J. *Circulation* **1996**, *94* (7), 1690.
(6) Gunn, J.; Cumberland, D. *Eur. Heart J.* **1999**, *20* (23), 1693.
(7) Whelan, D. M.; Van Der Giessen, W. J.; Krabbendam, S. C.; Van Vliet, E. A.; Verdouw, P. D.; Serruys, P. W.; Van Beusekom, H. M. M. *Heart* **2000**, *83* (3), 338.
(8) Drachman, D. E.; Edelman, E. R.; Seifert, P.; Groothuis, A. R.; Bornstein, D. A.; Kamath, K. R.; Palasis, M.; Yang, D. C.; Nott, S. H.; Rogers, C. *J. Am. Coll. Cardiol.* **2000**, *36* (7), 2325.
(9) Farb, A.; Heller, P. F.; Shroff, S.; Cheng, L.; Kolodgie, F. D.; Carter, A. J.; Scott, D. S.; Froehlich, J.; Virmani, R. *Circulation* **2001**, *104* (4), 473.
(10) Suzuki, T.; Kopia, G.; Hayashi, S.; Bailey, L. R.; Llanos, G.; Wilensky, R.; Klugherz, B. D.; Papandreou, G.; Narayan, P.; Leon, M. B.; Yeung, A. C.; Tio, F.; Tsao, P. S.; Falotico, R.; Carter, A. J. *Circulation* **2001**, *104* (10), 1188.
(11) Perin Emerson, C. *Rev. Cardiovasc. Med.* **2005**, *6* (Suppl 1), S13.
(12) Ranade, S. V.; Miller, K. M.; Richard, R. E.; Chan, A. K.; Allen, M. J.; Helmus, M. N. *J. Biomed. Mater. Res., Part A* **2004**, *71A* (4), 625.
(13) Colombo, A.; Moses, J. W.; Morice, M. C.; Ludwig, J.; Holmes, D. R.; Spanos, V.; Louvard, Y.; Desmedt, B.; Di Mario, C.; Leon, M. B. *Circulation* **2004**, *109* (10), 1244.
(14) Leon, M. B.; Moses, J. W.; Holmes, D. R.; Kereiakes, D. J.; Cutlip, D.; Cohen, S. A.; Kuntz, R. E. *J. Am. Coll. Cardiol.* **2005**, *45* (3), 49A.
(15) Kerner, A.; Gruberg, L.; Kapeliovich, M.; Grenadier, E. *Catheter. Cardiovasc. Interv.* **2003**, *60* (4), 505.
(16) Grube, E.; Silber, S.; Hauptmann, K. E.; Mueller, R.; Buellesfeld, L.; Gerckens, U.; Russell, M. E. *Circulation* **2003**, *107* (1), 38.
(17) Tanabe, K.; Serruys, P. W.; Grube, E.; Smits, P. C.; Selbach, G.; Van Der Giessen, W. J.; Staberock, M.; De Feyter, P.; Muller, R.; Regar, E.; Degertekin, M.; Ligthart, J. M. R.; Disco, C.; Backx, B.; Russell, M. E. *Circulation* **2003**, *107* (4), 559.
(18) Colombo, A.; Drzewiecki, J.; Banning, A.; Grube, E.; Hauptmann, K.; Silber, S.; Dudek, D.; Fort, S.; Schiele, F.; Zmudka, K.; Guagliumi, G.; Russell, M. E. *Circulation* **2003**, *108* (7), 788.
(19) Kim, J.; Parikh, N.; White, R. Future of the Coronary Stent Market: Who Will Win and Why? MIT Sloan School of Management course reading. http://ocw.mit.edu/NR/rdonlyres/Sloan-School-of-Management/15-912Spring-2005/3AA0ACA0-6D1F-4B76-8955-E5ED85293EA7/0/drug_el_s_te_stt.pdf (accessed December 4, 2006).
(20) Otsuka, Y.; Chronos, N. A. F.; Apkarian, R. P.; Robinson, K. A. *J. Invasive Cardiol.* **2007**, *19*, 71.
(21) Regar, E.; Sianos, G.; Serruys, P. W. *Br. Med. Bull.* **2001**, *59*, 227.
(22) Lahann, J.; Klee, D.; Thelen, H.; Bienert, H.; Vorwerk, D.; Hocker, H. *J. Mater. Sci.: Mater. Med.* **1999**, *10* (7), 443.
(23) Senkevich, J. J.; Yang, G. R.; Lu, T. M. *Colloids Surf., A* **2003**, *216* (1−3), 167.
(24) Hanefeld, P.; Westedt, U.; Wombacher, R.; Kissel, T.; Schaper, A.; Wendorff, J. H.; Greiner, A. *Biomacromolecules* **2006**, *7* (7), 2086.
(25) Lahann, J.; Klee, D.; Pluester, W.; Hoecker, H. *Biomaterials* **2001**, *22* (8), 817.
(26) Weiss, Z.; Mandler, D.; Shustak, G.; Domb, A. J. *J. Polym. Sci., Part A: Polym. Chem.* **2004**, *42* (7), 1658.
(27) Okner, R.; Oron, M.; Tal, N.; Mandler, D.; Domb, A. J. *Mater. Sci. Eng., C* **2007**, *27* (3), 510.
(28) Shustak, G.; Gadzinowski, M.; Slomkowski, S.; Domb, A. J.; Mandler, D. *New J. Chem.* **2007**, *31* (1), 163.
(29) Okner, R.; Domb, A. J.; Mandler, D. *Biomacromolecules* **2007**, *8* (9), 2928.
(30) Okner, R.; Oron, M.; Nyska, A.; Tal, N.; Kumar, N.; Mandler, D.; Domb, A. J. *J. Biomed. Mater. Res., Part A* **2009**, *88A* (2), 427.
(31) Mizrahi, B.; Shavit, R.; Domb, A. J. *J. Biomed. Mater. Res., Part B* **2008**, *86B* (2), 466.
(32) Taga, Y.; Kawai, K.; Nokubi, T. *J. Prosthet. Dent.* **2001**, *85* (4), 357.
(33) Liggins, R. T.; Hunter, W. L.; Burt, H. M. *J. Pharm. Sci.* **1997**, *86* (12), 1458.
(34) Konno, T.; Watanabe, J.; Ishihara, K. *J. Biomed. Mater. Res., Part A* **2003**, *65A* (2), 209.
(35) Burkstrand, J. M. *J. Vac. Sci. Technol.* **1982**, *20* (3), 440.
(36) Beck, F.; Michaelis, R. *J. Coat. Technol.* **1992**, *64* (808), 59.
(37) Noh, J. S.; Laycock, N. J.; Gao, W.; Wells, D. B. *Corros. Sci.* **2000**, *42* (12), 2069.
(38) Raval, A.; Choubey, A.; Engineer, C.; Kothwala, D. *Mater. Sci. Eng., A* **2004**, *386* (1−2), 331.
(39) Wolf, K. V.; Zong, Z.; Meng, J.; Orana, A.; Rahbar, N.; Balss, K. M.; Papandreou, G.; Maryanoff, C. A.; Soboyejo, W. *J. Biomed. Mater. Res., Part A* **2008**, *87A* (2), 272.
(40) Osterhold, M.; Wagner, G. *Prog. Org. Coat.* **2002**, *45* (4), 365.
(41) Migliavacca, F.; Petrini, L.; Montanari, V.; Quagliana, I.; Auricchio, F.; Dubini, G. *Med. Eng. Phys.* **2005**, *27* (1), 13.
(42) Burmeister, J. S.; Vrany, J. D.; Reichert, W. M.; Truskey, G. A. *J. Biomed. Mater. Res.* **1996**, *30* (1), 13.
(43) Lampin, M.; Warocquierclerout, R.; Legris, C.; Degrange, M.; Sigotluizard, M. F. *J. Biomed. Mater. Res.* **1997**, *36* (1), 99.
(44) Wang, Y. X.; Robertson, J. L.; Spillman, W. B.; Claus, R. O. *Pharm. Res.* **2004**, *21* (8), 1362.
(45) Cho, J. C.; Cheng, G. L.; Feng, D. S.; Faust, R.; Richard, R.; Schwarz, M.; Chan, K.; Boden, M. *Biomacromolecules* **2006**, *7* (11), 2997.
(46) Acharya, G.; Park, K. *Adv. Drug Delivery Rev.* **2006**, *58* (3), 387.
(47) Westedt, U.; Wittmar, M.; Hellwig, M.; Hanefeld, P.; Greiner, A.; Schaper, A. K.; Kissel, T. *J. Controlled Release* **2006**, *111*, 235.

AM800139S